Bimetallic Clusters Pt_6Au: Geometric and Electronic Structures within Density Functional Theory

Wei Quan Tian,*,† Maofa Ge,*,‡ Fenglong Gu,† and Yuriko Aoki†,§

Department of Material Sciences, Faculty of Engineering Sciences, Kyushu University, 6-1 Kasugakoen, Kasuga, Fukuoka, 816-8580, Japan, Institute of Chemistry, Chinese Academy of Sciences, Beijing 100080, People's Republic of China, and Group, PRESTO, Japan Science and Technology Agency (JST), Kawaguchi Center Building, Honcho 4-1-8, Kawaguchi, Saitama, 332-0012, Japan

Received: July 18, 2005; In Final Form: September 8, 2005

Within density functional theory at the general gradient approximation for exchange and correlation (BPW91) and the relativistic 19-electron Los Alamos National Laboratory effective core pseudopotentials and basis sets (3s3p2d), the geometric and electronic structures of Pt_6Au bimetallic clusters have been studied in detail in comparison with Pt_7. A total of 38 conformations for Pt_6Au are located. The most stable conformation for Pt_6Au is a sextet with an edge- and face-capped trigonal bipyramid, in which the Au atom caps an edge of the trigonal bipyramid. Pt_6Au, in general, prefers a three-dimensional geometry and high spin electronic state with multireference character. The electronic impact of the doping of Au in Pt clusters on the overall chemical activity of the doped bimetallic cluster is not as significant as that of the doping of Pt in Au clusters; however, the doping of Au lowers the chemical activity, thus enhancing the chemoselectivity in the gas phase, of PtAu bimetallic clusters.

I. Introduction

Bimetallic clusters are particularly important in catalytic applications[1] because of their unique catalytic selectivity,[2] which originates from their unique electronic structure[3] due to the interactions between the two different elements and their composition.[4] The PtAu bimetallic clusters (or alloys), which are important catalysts for alkane conversion,[5] C−N coupling,[4,6] isotope exchange,[7] and NO reduction,[8] were found to have enhanced catalytic activity.[9] The geometry of the PtAu bimetallic clusters is attributed to their unique electronic structure and properties. The investigation of the geometric and electronic structures of the core bimetallic cluster facilitates understanding on the metal cluster structure and its application.

Au clusters (with up to seven atoms) were found to prefer low spin and planar geometry while Pt clusters prefer high spin[10] and three-dimensional (3D) structure.[11] This is attributed to the strong relativistic effect of Au[10] in Au clusters and the involvement of Pt 5d and 6s atomic orbitals in bonding of Pt clusters.[11] The substitution of an Au atom by a Pt atom in Au_7 cluster does not change the essential structure of the Au cluster—the preference for two-dimensional (2D) geometry and low spin—although 3D structures of Au_6Pt are stable.[12] However, the electronic structure of Au_6Pt changes much upon the substitution of a Pt atom. The reactivity of Pt-doped Au cluster is much enhanced with respect to pure Au cluster.[13] In catalytic applications, Pt was found to be the essential catalytically active component in PtAu bimetallic catalysts.[4] Questions naturally arise: what are the geometric structure, electronic structure, and properties of Au-doped Pt clusters? Would the Au-doped Pt clusters keep a 3D structure and prefer high spin? What is the cause for the unique catalytic activity of AuPt bimetallic clusters? In bulky catalysts, Au generally acts as a poisoning reagent to catalytic activities;[1] similar behavior of Au can also be seen in clusters[14] and has been utilized for chemoselectivity of the PtAu clusters in some catalytic reactions.[14a] Detailed studies on the structures of these bimetallic clusters help in understanding their chemoselectivity in catalytic reactions. In the present work, we study the structure and properties of bimetallic cluster Pt_6Au in comparison with that of Pt_7 within density functional theory (DFT).[15] The structure of Pt_7 was studied in detail in our previous work.[11] The most stable conformation for Pt_7 has coupled tetragonal pyramid (CTP) geometry in quintet. The energy of septet CTP is also very close to quintet CTP.[11] Within the present general gradient approximation (GGA) of DFT, these two electronic states are degenerate.

II. Computational Details

The successful applications[11,12,16] of GGA due to Becke[17] and Perdew[18] for exchange and correlation functionals (BPW91) on transition metal clusters give us confidence in applying this method to the Pt_6Au cluster studies. The very strong relativistic effects of Au and Pt[19] have a profound impact on the structure, properties, and reactivity of Au or Pt clusters.[10,20] The relativistic 19-electron Los Alamos National Laboratory (LANL2DZ) effective core pseudopotentials[21] with the basis sets (3s3p2d) are employed in present studies to partially account for the relativistic effects. The optimized geometry for Pt_6Au cluster is further used to calculate the vibrational frequency to verify the nature of the stationary point on the potential energy surface (PES). If there is no imaginary frequency (no negative eigenvalue for the Hessian), the stationary point is a minimum. One and only one imaginary frequency for the stationary point indicates a transition state. More imaginary frequencies imply a high order saddle point on the PES. Since the structure and

* Corresponding authors. E-mail: wqtian@cube.kyushu-u.ac.jp (W.Q.T.); gemaofa@iccas.ac.cn (M.G.).
† Kyushu University.
‡ Chinese Academy of Sciences.
§ JST.

10.1021/jp053961e CCC: $30.25
Published on Web 10/12/2005

TABLE 1: Relative Stability, Ionization Potential, and Electron Affinity of Neutral Platinum Heptamer Predicted Using BPW91 Exchange-Correlation Functionals with LANL2DZ Relativistic Pseudopotentials and Gaussian Basis Set[a]

isomer	multiplicity	ΔE (eV)	IP (eV)	EA (eV)
CTP	5	0.00	7.12	2.76
	7	0.01	7.17	2.74
	3	0.10	7.11	2.82
	9	0.39	6.97	2.20
	1	0.40	5.18	4.88
ECTBP	3	0.16	8.98	3.00
	1	0.54	6.02	4.04
FCTBP	5	0.30	7.15	2.82
	3	0.31	7.10	2.86
	1	0.52	6.85	2.97
ECT	3	0.32 (TS)[b]		
	5	0.42 (SP)[b]		
FCOh	5	0.36	7.22	2.86
	3	0.39	7.23	2.76
TCT	3	0.54	7.09	2.88

[a] Only minima for the relevant clusters, except for ECT, are listed. Relative energies are from ref 13. [b] TS, transition state; SP, higher order saddle point.

properties of Pt_6Au cluster are the topics of present work, only minima are included in ongoing discussions. If a transition state (or high order saddle point) is very stable, the geometry of such a stationary point is distorted along the imaginary vibrational frequency modes to locate a minimum. Natural bond orbital (NBO)[22] analysis is performed for the electronic structure, natural atomic charge, and net spin analysis. For open shell electronic states, unrestricted DFT (UDFT) is employed in the calculations. Most of the calculations were carried out with Gaussian 98 (or Gaussian 03) quantum chemical packages.[23] For comparison, the relevant structures of Pt_7 to Pt_6Au are also analyzed.

III. Results and Discussion

Detailed studies on Pt_7 clusters can be found in ref 13. Only the relevant structures of Pt_7 to Pt_6Au are briefly discussed in the present work for comparison with Pt_6Au as shown in Figure 1S in the Supporting Information. The calculated relative energies, vertical ionization potential (IP), and electron affinity (EA)[24] of Pt_7 are listed in Table 1. The most stable conformation for Pt_7 is a quintet with CTP geometry. Septet CTP Pt_7 is nearly degenerate with quintet CTP. The energy of triplet CTP is also close to that of the quintet and septet CTP. Essentially, CTP Pt_7 has multireference character. Proper treatment of this conformation is beyond the scope of conventional DFT, although UDFT includes some multiconfigurational character. Nevertheless, the electronic structure from DFT studies certainly provides helpful information on transition metal clusters, since the prohibitive active space size of Pt_7 needed in multireference configuration interaction (MRCI) treatment rejects the application of MRCI in this case. The overall property of CTP Pt_7 can be the superposition of all the low-lying electronic states, especially the quintet and septet. The calculated IPs and EAs of these conformations are close to each other. However, the IPs and EAs of nonet and singlet CTP Pt_7 are different from those of the first three most stable electronic states. Nonet CTP Pt_7 has a smaller IP and EA, while singlet CTP Pt_7 has a smaller IP and larger EA, respectively, than those of the three most stable electronic states, thus indicating different electronic structures. The IPs and EAs of face-capped trigonal bipyramid (FCTBP) [FCTB in ref 11], face-capped "octahedron" (FCOh) [COh in ref 11], and tricapped tetrahedron (TCT) are close to those of quintet (and septet) CTP Pt_7, respectively. Edge-capped trigonal bipyramid (ECTBP) [ECTB in ref 13], however, has different IP and EA values. The IPs and EAs of transition metal clusters can be utilized along with other electronic properties to identify the structures of these clusters in experiment.

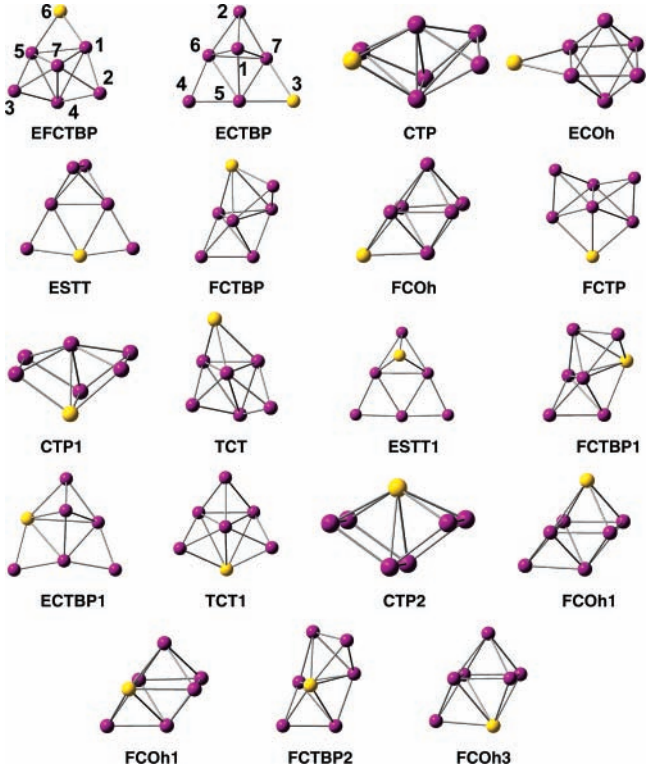

Figure 1. Structures of the Pt_6Au cluster. ECOh, edge-capped octahedron; FCTBP, face-capped trigonal bipyramid.

Substitution of a Pt atom by an Au atom in Pt_7 clusters drastically increases the conformations for the resultant Pt_6Au. A total of 38 minima have been located for Pt_6Au, as shown in Figure 1.[25] The relative energies, IPs, and EAs of the Pt_6Au minima are listed in Table 2.

The most stable conformation for Pt_6Au is a sextet with an edge- and face-capped trigonal bipyramid (EFCTBP) geometry in which the Au atom [Au(6) in Figure 1] caps an edge of the trigonal bipyramid. There is no structure in Pt_7 clusters corresponding to the EFCTBP Pt_6Au. Quadruplet EFCTBP Pt_6Au lies energetically close to the sextet EFCTBP, ca. 0.21 eV less stable than sextet EFCTBP Pt_6Au. The next close lying electronic state of EFCTBP is octet with 0.38 eV above the sextet EFCTBP. Decuplet EFCTBP has much higher energy than its lower counterparts with 1.55 eV lying above the sextet EFCTBP. Overall, the electronic state of EFCTB is of multireference with a mixture of sextet, quadruplet, and octet. The multireference character of the second most stable conformation, ECTBP, is even stronger than that of EFCTBP. In ECTBP Pt_6Au, the Au atom [Au(3) in Figure 1] caps an edge of the trigonal bipyramid. The energy of the lowest electronic state of ECTBP, sextet, is 0.17 eV higher than that of the sextet EFCTBP Pt_6Au. The quadruplet ECTBP is only 0.07 eV above the sextet ECTBP followed by the doublet ECTBP with energy only 0.02 eV higher than that of the quadruplet ECTBP. Most of the Pt_6Au clusters have multireference electronic states, e.g., CTP, edge-shared trapezoid and tetrahedron (ESTT), face-capped trigonal bipyramid (FCTBP), and FCOh, as shown in Figure 1. In fact, an electronic state with multireference character is normal in transition metal clusters with a partially filled d subshell. The doping of an Au atom does not change the

TABLE 2: Relative Stability, Ionization Potential, and Electron Affinity of the Neutral Bimetallic Cluster Pt_6Au Predicted Using BPW91 Exchange-Correlation Functionals with LANL2DZ Relativistic Pseudopotential and Gaussian Basis Set[a]

conformation	multiplicity	ΔE (eV)	IP (eV)	EA (eV)
EFCTBP	6	0.00	7.34	2.76
ECTBP	6	0.17	7.37	2.74
EFCTBP	4	0.21	7.91	2.99
ECTBP	4	0.24	7.45	3.09
ECTBP	2	0.26	7.51	3.04
CTP	6	0.36	7.22	2.72
ECOh	8	0.38	7.24	2.20
EFCTBP	8	0.38	6.85	2.14
ESTT	4	0.43	7.63	3.16
ECOh	2	0.47	7.44	2.53
CTP	4	0.49	7.17	2.80
FCOh	2	0.51	7.55	2.66
FCTBP	4	0.52	7.13	2.87
FCOh	4	0.54	7.07	2.85
CTP	2	0.55	7.45	2.94
FCTBP	2	0.56	7.20	2.99
FCTP	6	0.57	7.30	2.54
CTP1	4	0.57	7.20	2.93
CTP1	2	0.60	7.37	2.64
TCT	8	0.61	7.13	2.05
ESTT1	2	0.62	7.89	2.94
FCTBP1	2	0.63	7.33	2.91
ESTT	6	0.64	7.50	2.65
FCTBP1	4	0.64	7.06	2.93
TCT1	2	0.66	7.83	2.08
CTP2	6	0.69	7.17	2.83
FCOh1	4	0.69	7.17	2.93
ECTBP1	4	0.70	7.58	3.17
TCT1	4	0.70	7.29	2.78
FCOh2	4	0.73	7.07	2.95
FCOh3	2	0.73	7.51	2.53
FCTBP2	4	0.73	7.29	2.90
ESTT	2	0.76	7.91	2.99
CTP2	4	0.76	7.29	2.92
FCOh1	2	0.80	7.30	3.04
CTP2	2	0.81	7.64	2.75
EFCTBP	10	1.55	6.37	1.96
ESTT	8	2.32	6.55	2.28

[a] The relative energy (ΔE) is calculated with a zero point vibrational energy correction.

electronic structure of Pt_7 cluster much. This can be seen from the IP and EA values of Pt_6Au clusters. Overall, the IP and EA values of Pt_6Au clusters (as listed in Table 2) are close to those of corresponding Pt_7 (as listed in Table 1). However, the IP and EA values of Pt_6Au vary with the geometry of the cluster because of different bonding in different conformations. The vertical IPs and EAs should not be compared directly with experiment before corrections for the method's systematic error and geometric effect.

The close relative stabilities of Pt_6Au conformations make the experimental isolation of different isomers difficult. From the structure and relative energy of Pt_6Au, one can find that the coordination number of Au to Pt is less than that among the Pt atoms; e.g., the Au atom bonds to only two Pt atoms in EFCTBP and ECTBP Pt_6Au, the two most stable conformations. The bonding of Au atom in Pt_6Au is in contrast to the bonding of Pt atom in Au_6Pt clusters in which the Pt atom prefers as much bonding as possible with Au atoms.[12] The preference of low coordination of Au atom in Pt_6Au is also reflected in the doping of Au in CTP Pt_7 (the most stable conformation of Pt_7[11]) and COh Pt_7 (as shown in Figure 1S) at different positions. The most stable CTP Pt_6Au (CTP in Figure 1) is the one with least bonding of Au to Pt atoms; i.e., more Au coordination makes the conformation less stable. The different bonding characters

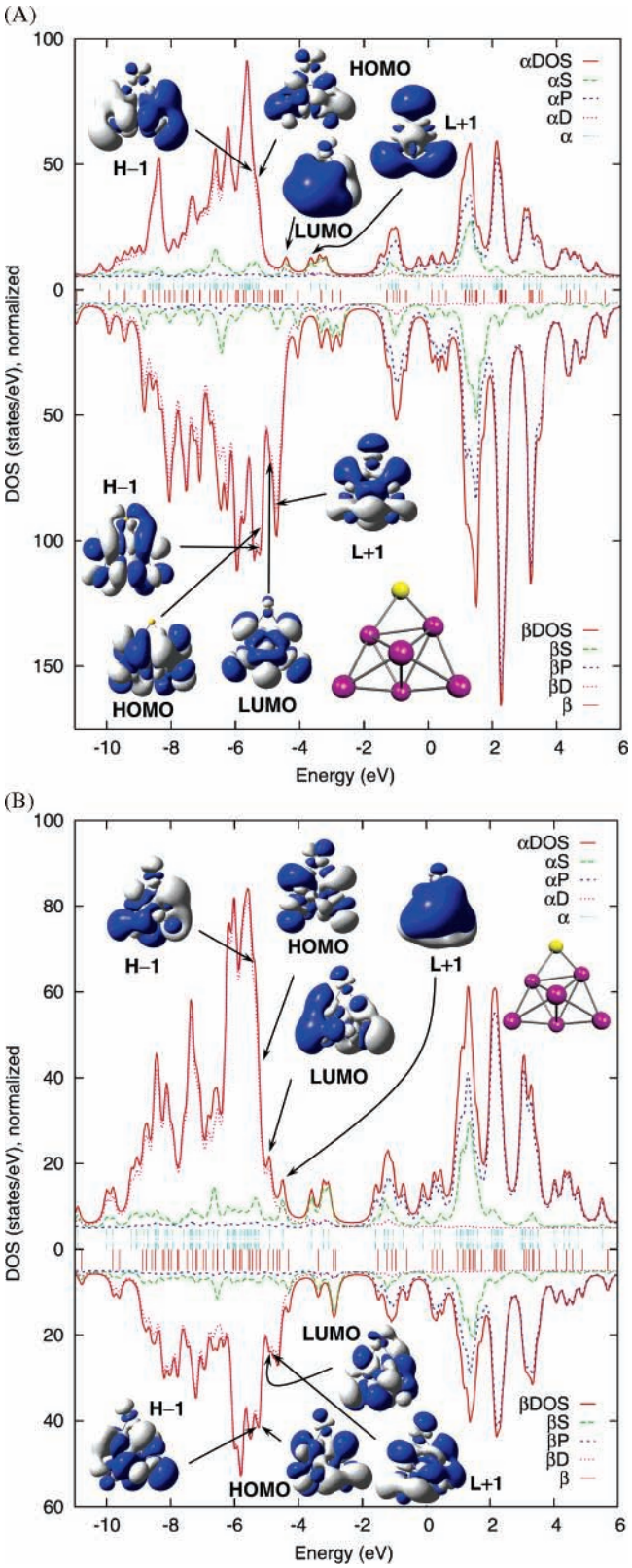

Figure 2. (A) One-electron energy spectrum, single electron density of states, and partial density of states of S, P, and D shells of EFCTBP Pt_6Au sextet (the yellow atom is Au). The surface isovalue for molecular orbital plotting is 0.01 $Å^{-3}$. (B) One-electron energy spectrum, single electron density of states, and partial density of states of S, P, and D shells of EFCTBP Pt_6Au quadruplet (the yellow atom is Au). The surface isovalue for molecular orbital plotting is 0.01 $Å^{-3}$.

of Au and Pt atoms in bimetallic PtAu clusters are ascribed to the different shell structures of Au and Pt atoms: the 5d subshell of Au is full (Au: $5d^{10}6s^1$) while Pt has one partially occupied

TABLE 3: Electronic Configurations, Natural Atomic Charges, and Spin Densities of the Most Stable Minima of the Pt_6Au Bimetallic Clusters[a]

atom	EFCTBP Pt_6Au [6]	charge (spin)	ECTBP Pt_6Au [6]	charge (spin)
1	$5d^{9.11}6s^{0.88}6p^{0.04}6d^{0.01}7p^{0.01}$	−0.06 (0.81)	$5d^{9.04}6s^{0.67}6p^{0.04}$	0.25 (0.88)
2	$5d^{9.08}6s^{1.00}6p^{0.03}$	−0.11 (0.85)	$5d^{9.12}6s^{0.98}6p^{0.03}$	−0.13 (0.68)
3	$5d^{9.08}6s^{1.00}6p^{0.03}$	−0.11 (0.85)	$5d^{9.83}6s^{1.21}6p^{0.01}$	−0.05 (0.06)
4	$5d^{9.06}6s^{0.70}6p^{0.05}7p^{0.01}$	0.19 (0.81)	$5d^{9.00}6s^{1.12}6p^{0.02}$	−0.13 (0.81)
5	$5d^{9.11}6s^{0.88}6p^{0.04}6d^{0.01}7p^{0.01}$	−0.06 (0.81)	$5d^{8.97}6s^{0.96}6p^{0.05}6d^{0.02}7p^{0.01}$	−0.01 (0.92)
6	$5d^{9.81}6s^{1.22}6p^{0.01}$	−0.05 (0.07)	$5d^{9.01}6s^{0.89}6p^{0.04}6d^{0.01}7p^{0.01}$	0.05 (0.85)
7	$5d^{9.06}6s^{0.70}6p^{0.05}7p^{0.01}$	0.19 (0.81)	$5d^{9.06}6s^{0.85}6p^{0.05}7p^{0.01}$	0.03 (0.80)
atom	EFCTBP Pt_6Au [4]	charge (spin)	ECTBP Pt_6Au [4]	charge (spin)
1	$5d^{9.08}6s^{0.89}6p^{0.04}6d^{0.01}7p^{0.01}$	−0.03 (0.75)	$5d^{9.05}6s^{0.65}6p^{0.05}$	0.26 (0.46)
2	$5d^{9.11}6s^{0.96}6p^{0.03}$	−0.10 (0.54)	$5d^{9.10}6s^{1.03}6p^{0.03}$	−0.16 (0.38)
3	$5d^{9.12}6s^{0.96}6p^{0.03}$	−0.11 (0.12)	$5d^{9.81}6s^{1.23}6p^{0.01}$	−0.06 (0.03)
4	$5d^{9.05}6s^{0.72}6p^{0.04}7p^{0.01}$	0.19 (0.85)	$5d^{9.00}6s^{1.12}6p^{0.02}$	−0.14 (0.43)
5	$5d^{9.08}6s^{0.90}6p^{0.04}6d^{0.01}7p^{0.01}$	−0.04 (0.76)	$5d^{9.06}6s^{0.94}6p^{0.04}6d^{0.01}7p^{0.01}$	−0.07 (0.46)
6	$5d^{9.81}6s^{1.25}6p^{0.01}$	−0.06 (0.06)	$5d^{8.97}6s^{0.86}6p^{0.05}6d^{0.01}7p^{0.01}$	0.11 (0.37)
7	$5d^{9.08}6s^{0.71}6p^{0.04}7p^{0.01}$	0.17 (−0.08)	$5d^{9.04}6s^{0.85}6p^{0.05}6d^{0.01}7p^{0.01}$	0.05 (0.88)
atom	ECTBP Pt_6Au [2]	charge (spin)		
1	$5d^{9.06}6s^{0.65}6p^{0.04}$	0.24 (−0.59)		
2	$5d^{9.09}6s^{1.01}6p^{0.03}$	−0.13 (−0.13)		
3	$5d^{9.81}6s^{1.23}6p^{0.01}$	−0.04 (0.03)		
4	$5d^{8.97}6s^{1.12}6p^{0.02}$	−0.11 (0.67)		
5	$5d^{9.02}6s^{0.96}6p^{0.05}6d^{0.01}7p^{0.01}$	−0.04 (0.79)		
6	$5d^{9.02}6s^{0.84}6p^{0.04}6d^{0.01}7p^{0.01}$	0.08 (0.19)		
7	$5d^{9.09}6s^{0.84}6p^{0.05}6d^{0.01}7p^{0.01}$	0.01 (0.04)		

[a] The core electrons are not shown. The labels of atoms in each structure are shown in Figure 2. The multiplicity of each conformation is specified in square brackets. The values in parentheses are the net spin of each atom.

5d orbital (Pt: $5d^9 6s^1$). The multicoordination of Au is mainly due to its strong relativistic effect, which involves partial bonding of 5d orbitals.[10,19] Similar to Pt_7, Pt_6Au prefers electronic states with high multiplicity as shown in Table 2.

The electronic configurations, natural atomic charges, and net spins from NBO of the five most stable conformations of Pt_6Au are listed in Table 3 for further study on their electronic structures. In the electronic structures for the five Pt_6Au conformations, charge transfer occurs from Pt to Au. Most of the net spin distributes on Pt atoms in all conformations. The intraatomic charge transfer occurs from 5d to 6s in the Au atom, while it occurs in the reverse direction in the Pt atoms. The electron promotion from 5d to 6s in Au is so conspicuous that it clearly indicates the significant involvement of 5d orbital in bonding. Between the two close lying electronic states of EFCTBP, sextet and quadruplet, the electronic configurations and charge distributions of these two states are similar. Pt(4) and Pt(7) (the atomic labels are shown in Figure 1) have the largest positive charge, while Pt(2) and Pt(3) have the most electrons in these two electronic states of the EFCTBP Pt_6Au. In both electronic states, most of the net spin resides on Pt(1), Pt(4), and Pt(5). From the quadruplet to the sextet EFCTBP Pt_6Au, the drastic change of net spin distribution occurs on Pt(7) (from −0.08 [β spin] to 0.81 [α spin]), thus a suggesting structural change from quadruplet to sextet. The similarity of the electronic configurations and charge distributions of different electronic states is also found among the three most stable electronic states of ECTBP—sextet, quadruplet, and doublet—which explains the possible mixing of these electronic states in the wave function of the ECTBP Pt_6Au. The largest charge distribution change with electronic state among the three states of the ECTBP Pt_6Au is the net charge on Pt(6). The most noticeable change in net spin on each atom with the change of electronic state is the net spin on Pt(1) (from −0.59 [β spin] to 0.46 [α spin]) and Pt(2) (from −0.13 [β spin] to 0.38 [α spin]) from the doublet to the quadruplet ECTBP Pt_6Au. In all five electronic states of EFCTBP and ECTBP, the net spin on the Au atom is close to zero and it does not change much with electronic state.

Density of states (DOS) and partial density of states (PDOS), in combination with molecular orbital (MO), especially frontier MOs, give the overall electronic structure and reactivity of a system. The DOS, PDOS, and frontier MOs of the EFCTBP sextet and the quadruplet Pt_6Au are plotted in Figure 2. These two electronic states have similar overall electronic structures while details differ. Both electronic states have relatively clear d, s, and p bands with a very small highest occupied molecular orbital and lowest unoccupied molecular orbital (HOMO−LUMO) gap which renders excited states feasibly accessible. The bonding of the cluster is mainly from 5d atomic orbitals. The major hybridization (5d6s hybridization) occurs at the frontier orbital region responsible for the cluster bonding, although its role is limited. 6s6p hybridization occurs at a higher energy region, and it has no significant impact on the chemistry of the clusters. The contribution to the frontier MOs from Au is limited in both electronic states, and this is consistent with the net spin distribution in the cluster. With more unpaired electrons, the sextet EFCTBP Pt_6Au has more split bands. It also has more symmetric MOs, thus indicating a more symmetric nuclear frame, than the quadruplet ECFTBP Pt_6Au.

The overall electronic structures for the ECTBP Pt_6Au clusters are similar to those of the EFCTBP Pt_6Au. However, the detailed electronic structure, thus chemical activity, of these clusters changes with the nuclear frame. All the DOS, the PDOS, and the frontier MOs for sextet, quadruplet, and doublet ECTBP Pt_6Au as well as the overlap population density of states (OPDOS)[26] are plotted in Figures 3, 4, and 5, respectively. OPDOS depicts bonding between two groups in a system, and it is employed in the present work to study different bonding between Pt and Au in the Pt_6Au cluster. Only the HOMO−1, the HOMO, the LUMO, and the LUMO+1 are plotted for chemical reactivity since usually the frontier MOs are most active in chemical reaction. The contribution of the frontier MOs from the Au atom is clearly manifested by the MOs in the three

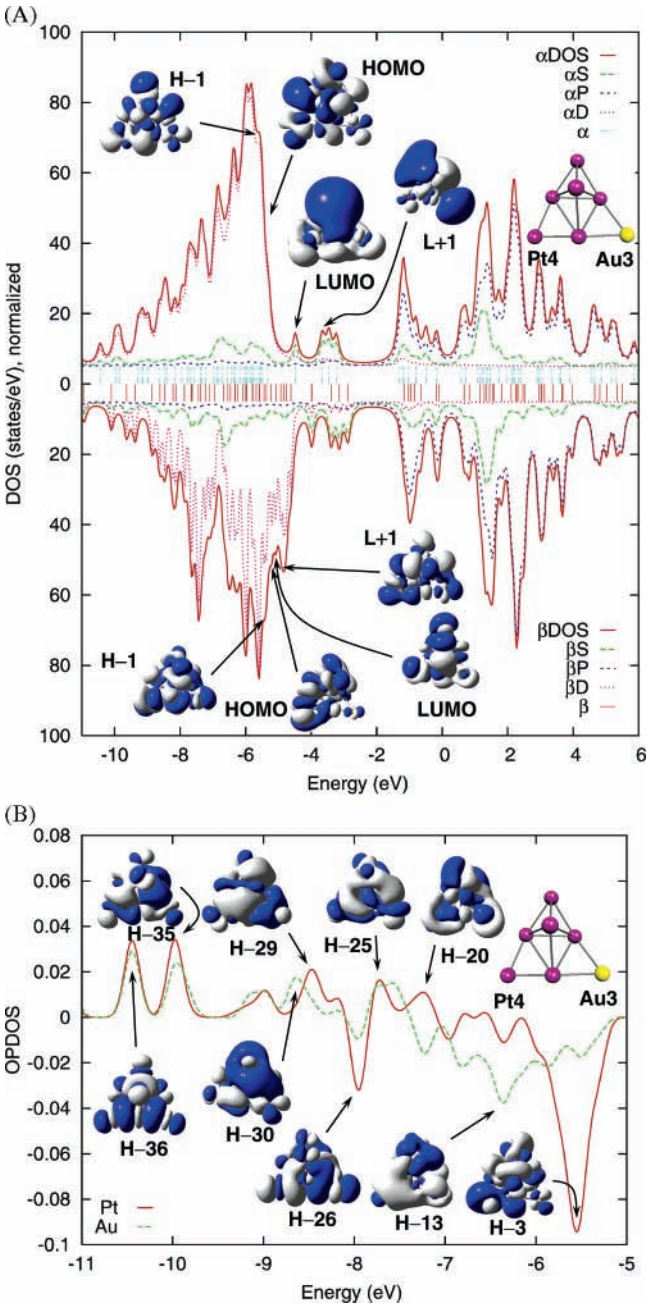

Figure 3. (A) One-electron energy spectrum, single electron density of states, and partial density of states of S, P, and D shells, and frontier molecular orbitals of ECTBP Pt_6Au sextet. The surface isovalue for molecular orbital plotting is 0.01 $Å^{-3}$. (B) The overlap population density of states between Pt(4) and the rest of the cluster, between Au(3) and the rest of the Pt atoms in ECTBP Pt_6Au sextet from Mulliken population analysis, and some occupied molecular orbitals. The surface isovalue for the molecular orbital plotting is 0.01 $Å^{-3}$.

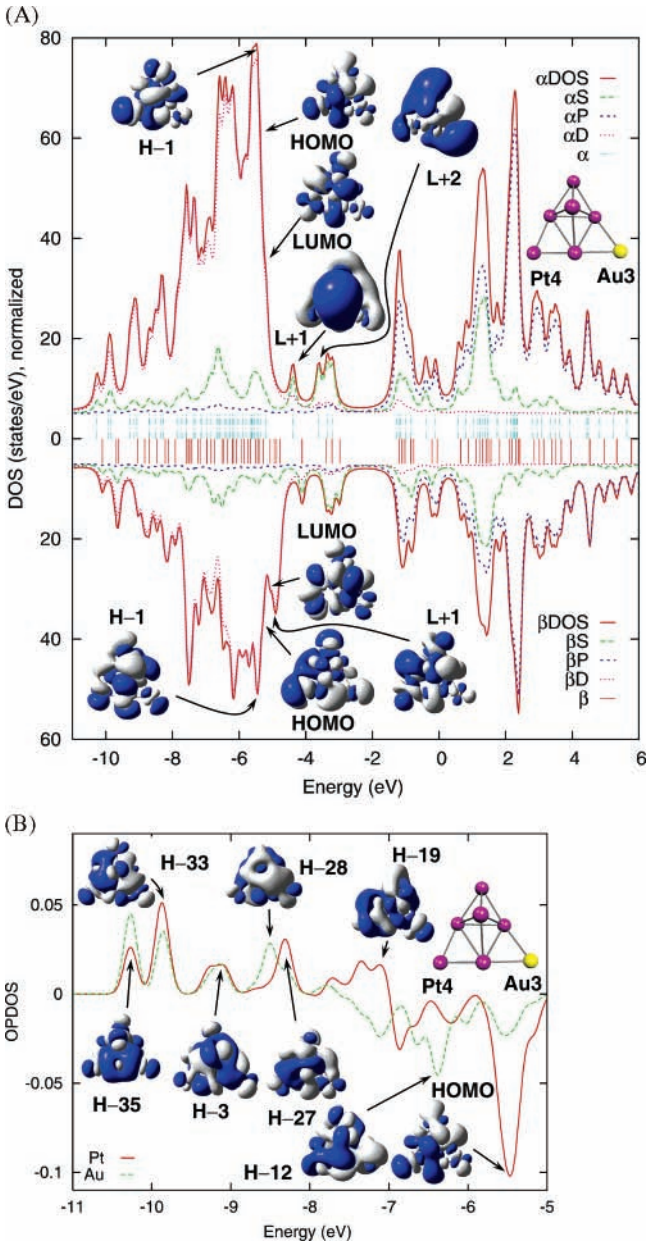

Figure 4. (A) One-electron energy spectrum, single electron density of states, and partial density of states of S, P, and D shells, and frontier molecular orbitals of ECTBP Pt_6Au quadruplet. The surface isovalue for molecular orbital plotting is 0.01 $Å^{-3}$. (B) The overlap population density of states between Pt(4) and the rest of the cluster, between Au(3) and the rest of the Pt atoms in the ECTBP Pt_6Au quadruplet from Mulliken population analysis, and some occupied molecular orbitals. The surface isovalue for molecular orbital plotting is 0.01 $Å^{-3}$.

figures. Au obviously has much less contribution to the frontier MOs than its counterpart atom Pt(4) does; thus Au lowers the reactivity of Pt clusters through spreading on the Pt cluster (or alloy) surface. This qualitatively explains the poisoning role that Au plays in the Pt catalytic reaction. The lowering of catalytic activity of PtAu clusters by Au, on the other hand, refines the chemoselectivity of PtAu clusters since different reaction channels have different reaction mechanisms thus with different sensitivities to the catalyst. The doping of Au breaks the symmetry of the MOs of the bimetallic cluster with respect to the MOs of the ECTBP Pt_7 as shown in Figure 5B. Similar to the case of the EFCTBP Pt_6Au, the overall electronic structure and chemical activity of the ECTBP Pt_6Au is a mixture (or superposition) of all three closely low-lying electronic states. According to the frontier MOs, the net spin, and the charge distribution in the ECTBP Pt_6Au, the chemical activity of the ECTBP Pt_6Au is similar to, while lower than, that of ECTBP Pt_7.[11]

OPDOS analysis helps in studying the detailed bonding between a group of atoms and the other atoms in a system. The OPDOS of all three lowest electronic states of the ECTBP Pt_6Au, as well as the OPDOS of the ECTBP Pt_7 for comparison, are plotted in Figures 3B, 4B, 5B, and 5C. Triplet ECTBP Pt_7 has C_s symmetry as manifested by its MOs in Figure 5C. The two capping Pt atoms to the trigonal bipyramid in the ECTBP Pt_7 have strong bonding MOs below −9.0 eV and have

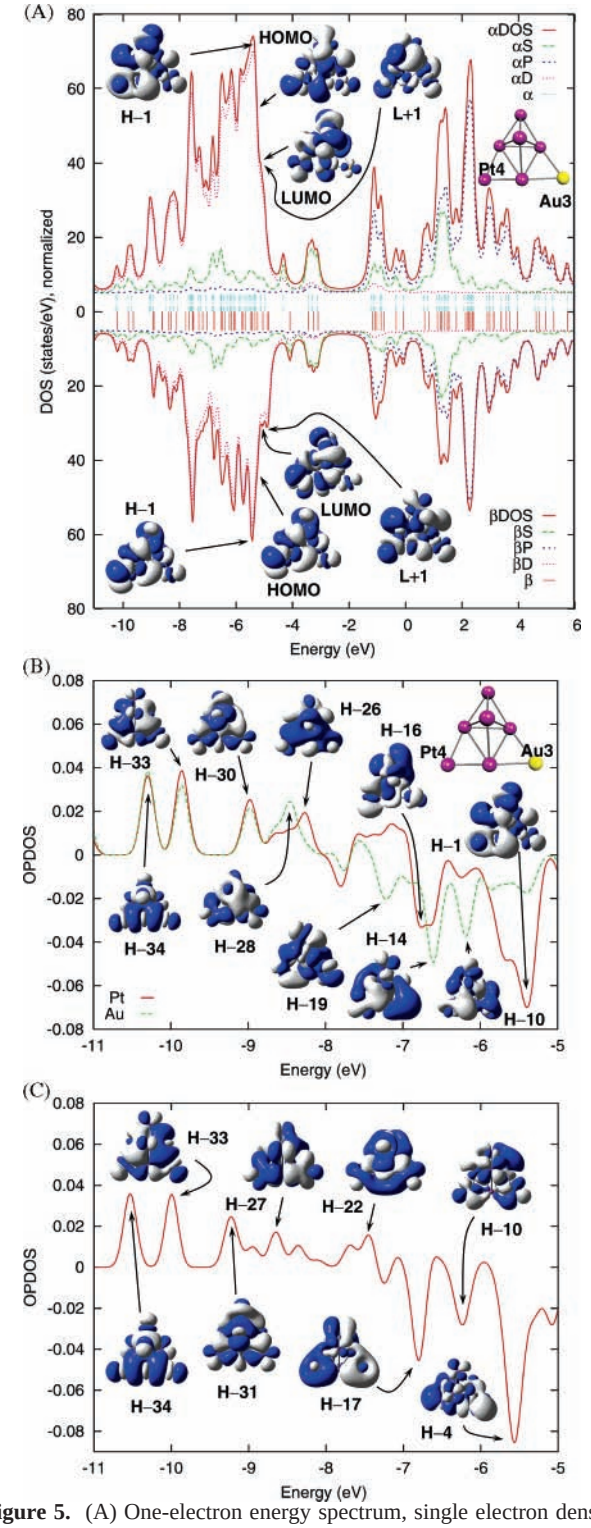

Figure 5. (A) One-electron energy spectrum, single electron density of states, partial density of states of S, P, and D shells, and frontier molecular orbitals of ECTBP Pt_6Au doublet. The surface isovalue for molecular orbital plotting is 0.01 $Å^{-3}$. (B) The overlap population density of states between Pt(4) and the rest of the cluster, between Au(3) and the rest of the Pt atoms in the ECTBP Pt_6Au doublet from Mulliken population analysis, and some occupied molecular orbitals. The surface isovalue for the molecular orbital plotting is 0.01 $Å^{-3}$. (C) The overlap population density of states between the edge-capping Pt-(4) [or Pt(3)] and the rest of the cluster, in the ECTBP Pt_7 septet from Mulliken population analysis, and some occupied molecular orbitals. The labels of atoms are the same as for the ECTBP Pt_6Au in Figure 2. The surface isovalue for molecular orbital plotting is 0.01 $Å^{-3}$.

antibonding with the rest of the Pt atoms above −7.0 eV. There is a strong antibonding MO (HOMO−4) ca. 5.40 eV. The region from −9.0 to −7.0 eV is essentially nonbonding for the edge-capping Pt atoms. In the ECTBP Pt_6Au, the remaining edge-capping Pt [Pt(4) in Figures 3−5] atom has roughly similar bonding with the rest of the cluster as it does in the ECTBP Pt_7. The conspicuous change in the bonding of atom Pt(4) in the ECTBP Pt_6Au occurs in the nonbonding and antibonding regions ca. from −9.0 to −6.0 eV. In the antibonding region (−7.0 to −5.0 eV) for Pt(4), there are three major peaks in the ECTBP Pt_7: the HOMO−17 (−6.80 eV), the HOMO−10 (−6.20 eV), and the HOMO−4 (−5.40 eV). In the doublet ECTBP Pt_6Au, the antibonding peak at −6.20 eV disappears for the edge-capping Pt atom while the Au atom retains these two antibonding peaks. These first two antibonding peaks of Pt(4) from the lower energy side disappear in the sextet and the quadruplet ECTBP Pt_6Au. In all three electronic states of the ECTBP Pt_6Au, the antibonding peak at −5.4 eV in Pt_7 remains. This peak is the strongest antibonding MO of Pt(4) in all three electronic states of the ECTBP Pt_6Au. The most noticeable change in the bonding of Pt(4) in the ECTBP Pt_6Au with respect to its counterpart in the ECTBP Pt_7 is in the region of nonbonding (from −9.0 to −7.0 eV): in the doublet ECTBP Pt_6Au, the nonbonding region comes with a small antibonding peak at −7.80 eV, there is an enhanced bonding peak at −8.32 eV for Pt(4) in the quadruplet ECTBP Pt_6Au, and a new antibonding peak appears at −7.95 eV in the sextet ECTBP Pt_6Au. The bonding of Au atom to Pt atoms is similar to that of the counterpart Pt atom in the low-energy region ca. −11.0 to −9.0 eV in all the structures, while it changes in the region above −9.0 eV. The details of bonding and antibonding of the Au atom as well as the edge-capping Pt atom can be inferred from the MOs in Figures 3−5.

III. Concluding Remarks

Within DFT, the detailed geometric and electronic structures of the bimetallic cluster Pt_6Au have been extensively studied and compared with those of the pure Pt_7 cluster. In conclusion, the following significant contributions toward understanding the structure and properties of PtAu clusters are concluded:

1. Like the Pt_7 cluster, the Pt_6Au prefers high spin electronic states and 3D geometry.

2. In contrast to the bonding of Pt in Au_6Pt,[12] Au prefers low coordination with Pt atoms in Pt_6Au.

3. According to the frontier MOs of Pt_6Au, the contribution from the Au atom to the chemical activity of PtAu cluster is limited. This partially explains, in combination with 2, the poisoning role of Au in Pt-catalyzed reaction. On the other hand, the lowering of reactivity by Au in PtAu cluster brings new chemoselectivity in PtAu clusters, broadening the application of PtAu bimetallic clusters.

The relative stabilities of the Pt_6Au clusters lie very close to each other, thus causing difficulty in isolating the Pt_6Au conformation in experiment. The present DFT exploration on the structures of the Pt_6Au clusters provides helpful information on the synthesis of Pt_6Au complex and chemical application of the Pt_6Au clusters. However, since the electronic states of Pt_6Au are very close to each other, a more proper and accurate prediction on this cluster awaits a method capable of handling multireference wave functions.

Acknowledgment. W.Q.T. thanks the Japan Society for the Promotion of Science for financial support. M.F.G. thanks the foundation of the Hundred Persons Talents. Y.A. and F.L.G. are grateful to Research and Development Applying Advanced Computational Science and Technology of the Japan Science

and Technology Agency (ACT-JST) and the Ministry of Education, Culture, Sports, Science and Technology (MEXT) for financial support.

Supporting Information Available: Structures of relevant Pt_7 clusters and saddle points for Pt_6Au from Gaussian calculations. IR spectra of the 38 Pt_6Au conformations in Table 2. This material is available free of charge via the Internet at http://pubs.acs.org.

References and Notes

(1) Sinfelt, J. H. *Bimetallic Catalysis: Discoveries, Concepts, and Applications*; Wiley: New York, 1983.

(2) Mihut, C.; Descorme, C.; Duprez, D.; Amiridis, M. D. *J. Catal.* **2002**, *212*, 125.

(3) Chandler, B. D.; Schabel, A. B.; Blandford, C. F.; Pignolet, L. H. *J. Catal.* **1999**, *187*, 367.

(4) Koszinowski, K.; Schröder, D.; Schwarz, H. *Organometallics* **2004**, *23*, 1132.

(5) Chandler, B. D.; Schabel, A. B.; Pignolet, L. H. *J. Catal.* **2000**, *193*, 186.

(6) Koszinowski, K.; Schröder, D.; Schwarz, H. *J. Am. Chem. Soc.* **2003**, *125*, 3676.

(7) (a) Aubart, M. A.; Pignolet, L. H. *J. Am. Chem. Soc.* **1992**, *114*, 7901. (b) Aubart, M. A.; Dor Koch, J. F.; Pignolet, L. H. *Inorg. Chem.* **1994**, *33*, 3852.

(8) Mihut, C.; Chandler, B. D.; Amiridis, M. D. *Catal. Commun.* **2002**, *3*, 91.

(9) Yeates, R. C.; Somorjai, G. A. *J. Catal.* **1987**, *103*, 208.

(10) Häkkinen, H.; Moseler, M.; Landman, U. *Phys. Rev. Lett.* **2002**, *89*, 033401.

(11) Tian, W. Q.; Ge, M.; Sahu, B. R.; Wang, D. X.; Yamada, T.; Mashiko, S. *J. Phys. Chem. A* **2004**, *108*, 3806.

(12) Tian, W. Q.; Ge, M.; Aoki, Y.; Gu, F.; Yamada, T. Submittted for publication in *J. Phys. Chem. A.*

(13) Yuan, Y.; Asakura, K.; Wan, H.; Tsai, K.; Iwasawa, Y. *J. Mol. Catal. A* **1997**, *122*, 147.

(14) (a) Koszinowski, K.; Schröder, D.; Schwarz, H. *ChemPhysChem* **2003**, *4*, 1233. (b) Cruz, A.; del Angel, G.; Poulain, E.; Martinez-Magadan, J. M.; Castro, M. *Int. J. Quantum Chem.* **1999**, *75*, 699.

(15) (a) Hohenberg, P.; Kohn, W. *Phys. Rev.* **1964**, *136*, B864. (b) Kohn, W.; Sham, L. J. *Phys. Rev.* **1965**, *40*, A1133. (c) Parr, R. G.; Yang, W. *Density-functional theory of atoms and molecules*; Oxford University Press: New York, 1989.

(16) (a) Wang, X.; Andrews, L. *J. Phys. Chem. A* **2001**, *105*, 5812. (b) Andrews, L.; Wang, X.; Manceron, L. *J. Chem. Phys.* **2001**, *114*, 1559.

(17) Becke, A. D. *Phys. Rev. A* **1988**, *38*, 3098.

(18) (a) Perdew, J. P.; Chevary, J. A.; Vosko, S. H.; Jackson, K. A.; Pederson, M. R.; Singh, D. J.; Fiolhais, C. *Phys. Rev. B* **1992**, *46*, 6671. (b) Perdew, J. P.; Burke, K.; Wang, Y. *Phys. Rev. B* **1996**, *54*, 16533.

(19) Pyykkö, P. *Chem. Rev.* **1988**, *88*, 563.

(20) Schwarz, H. *Angew. Chem., Int. Ed.* **2003**, *42*, 4442.

(21) Hay, P. J.; Wadt, W. R. *J. Chem. Phys.* **1985**, *82*, 299.

(22) Reed, A. E.; Curtiss, L. A.; Weinhold, F. *Chem. Rev.* **1988**, *88*, 899.

(23) *Gaussian 98*, revision A.7; Gaussian, Inc.: Pittsburgh, PA, 1998. *Gaussian 03*, revision C.02; Gaussian, Inc.: Wallingford CT, 2004 (www.gaussian.com).

(24) The IP and EA are calculated from the geometry of the neutral structure. The multiplicity of cation in IP calculation is the one right below that of the neutral cluster, and the multiplicity of anion in EA calculation is the one right above the neutral cluster. This might be different from experimental observation due to the stability of cations and anions.

(25) Only minima for Pt_6Au are listed. The structures of saddle points are listed in the Supporting Information. To help to identify the Pt_6Au isomers in the experiment, the infrared spectra of all minima are plotted in the Supporting Information.

(26) (a) Hoffmann, R. *Solids and Surfaces: A Chemist's View of Bonding in Extended Structures*; Wiley-VCH Inc.: New York, 1988. (b) The overlap population densities of states for all structures were plotted with GaussSum: O'Boyle, N. M.; Vos, J. G. *GaussSum 0.9*; Dublin City University, 2005. Available at http://gausssum.sourceforge.net.